*International Journal of Thermophysics, Vol. 7, No. 1, 1986*

# Vapor–Liquid Equilibrium of Near-Critical Binary Alkane Mixtures[1]

**J. C. Rainwater[2] and F. R. Williamson[2]**

The modified Leung–Griffiths model of Rainwater and Moldover is used to correlate vapor–liquid equilibrium (VLE) surfaces in pressure, temperature, and density for binary mixtures in the near-critical region. The systems studied are butane–pentane, propane–isopentane, butane–hexane, and ethane–butane. The model, which has also successfully fit several other mixtures, is based on scaling-law equations of state expressed in terms of field variables. It incorporates a variation of the principle of corresponding states as well as the coupling of density and composition change across the phase boundary. As the width of the dew-bubble curves increases, additional parameters are required to obtain successful VLE correlations.

**KEY WORDS:** binary mixtures; butane; critical region; field variables; hexane; isopentane; pentane; propane; vapor–liquid equilibrium.

## 1. THE THERMODYNAMIC MODEL

This paper reports some further results of an ongoing project to correlate the vapor–liquid equilibrium (VLE) of binary mixtures in the critical region. The thermodynamic model is that of Leung and Griffiths [1] as modified by Moldover, Rainwater, and co-workers [2–5]. Only a very abbreviated description of the model is described here. Further details, including its thermodynamic foundations, have been presented elsewhere [2–5].

The system of interest is a binary mixture whose coexistence surface in the pressure–temperature ($P$–$T$) plane is bounded from the sides by the pure fluid vapor pressure curves and from above by a continuous critical

---

[1] Paper presented at the Ninth Symposium on Thermophysical Properties, June 24–27, 1985, Boulder, Colorado, U.S.A.

[2] Thermophysics Division, National Bureau of Standards, Boulder, Colorado 80303, U.S.A.

0195-928X/86/0100-0065$05.00/0

line. The coordinates of the coexistence region defined by the model are $\zeta$ and $t$, where

$$\zeta = \frac{e^{\mu_1/RT}}{Ke^{\mu_2/RT} + e^{\mu_1/RT}} \tag{1}$$

$$t = \frac{T - T_c(\zeta)}{T_c(\zeta)} \tag{2}$$

where $\mu_i$ is the chemical potential of fluid $i$, $R$ is the gas constant, $K$ is an arbitrary constant, and $T_c$ is the composition-dependent critical temperature. Our convention is that fluid 1 has the higher critical temperature and the (molar) composition $x$ equals zero for pure fluid 1 and one for pure fluid 2. From the divergence of $\mu_i$ at infinite dilution, $\zeta = 1$ at $x = 0$ and $\zeta = 0$ at $x = 1$. A basic assumption of the model is that, along the critical line, $x = 1 - \zeta$.

The mapping from $\{P, T\}$ to $\{\zeta, t\}$ is given by

$$\frac{P\,T_c(\zeta)}{T\,P_c(\zeta)} = 1 + C_3(\zeta)(-t)^{1.9} + C_4(\zeta)\,t + C_5(\zeta)\,t^2 + C_6(\zeta)\,t^3 \tag{3}$$

Here $P_c$ is the composition-dependent critical pressure, and

$$C_i(\zeta) = C_i^{(2)} + \zeta C_i' \tag{4}$$

$$C_i' = C_i^{(1)} - C_i^{(2)} \tag{5}$$

where the coefficients $C_i^{(j)}$ are determined from fits to the vapor-pressure curves of the respective pure fluids.

The objective is to predict, for a given thermodynamic state point $\{\zeta, t\}$, the coexisting liquid and vapor densities $\rho_l$ and $\rho_v$ and the coexisting liquid and vapor compositions $x_l$ and $x_v$, given the pure fluid saturation properties, the critical line in $T$, $P$, and $\rho$, and a minimal number of additional adjustable parameters. The model yields the following solutions:

$$\rho/\rho_c(\zeta) = 1 \pm C_1(\zeta)(-t)^{0.355} + C_2(\zeta)\,t \tag{6}$$

$$x_j = (1-\zeta)\left\{1 - \zeta\left[\frac{\bar{Q}(\zeta, t)}{\rho_j} - \frac{\bar{Q}(\zeta, 0)}{\rho_c} - \bar{H}(\zeta, t)\right]\right\} \tag{7}$$

where $\rho_c$ is the composition-dependent critical density, plus refers to be liquid and minus to the vapor, and $j = l$, v. The quantities $\bar{Q}$ and $\bar{H}$ are defined as follows.

$$\begin{aligned}\bar{Q}(\zeta, t) &= \frac{PT_c}{RTP_c}\frac{d}{d\zeta}\frac{P_c}{T_c} + \frac{P_c}{RT_c}\left[C_3'(-t)^{1.9} + C_4't + C_5't^2 + C_6't^3\right] \\ &\quad + \frac{P_c}{R}\frac{d(1/T_c)}{d\zeta}(1+t)\left[-1.9\, C_3(-t)^{0.9} + C_4 + 2C_5t + 3C_6t^2\right]\end{aligned} \tag{8}$$

$$\bar{H}(\zeta, t) = C_H(1 + C_z t)\frac{d\ln T_c}{d\zeta} \tag{9}$$

where $P_c$, $T_c$, and $C_i$ are $\zeta$ dependent, and $C_2(\zeta)$ obeys Eqs. (4) and (5) but

$$C_1(\zeta) = \frac{C_1^{(2)} + \zeta\left[C_1^{(1)} - C_1^{(2)}\right]}{1 + C_X\zeta(1-\zeta)\,|\bar{Q}(\zeta, 0)|/\rho_c(\zeta)} \tag{10}$$

To complete the model, the critical line is fit to polynomials constrained to the appropriate pure fluid critical properties at the limits $x = 0$ and $x = 1$.

$$\frac{1}{RT_c(x)} = \frac{1-x}{RT_{c1}} + \frac{x}{RT_{c2}} + x(1-x)\left[T_1 + (1-2x)\,T_2 + (1-2x)^2\,T_3\right] \tag{11}$$

$$\begin{aligned}\frac{P_c(x)}{RT_c(x)} &= \frac{(1-x_T)\,P_{c1}}{RT_{c1}} + \frac{x_TP_{c2}}{RT_{c2}} \\ &\quad + x_T(1-x_T)\left[\bar{P}_1 + (1-2x_T)\,\bar{P}_2 + (1-2x_T)^2\,\bar{P}_3\right]\end{aligned} \tag{12}$$

$$\begin{aligned}\rho_c(x) &= (1-x_T)\,\rho_{c1} + x_T\rho_{c2} \\ &\quad + x_T(1-x_T)\left[\bar{\rho}_1 + (1-2x_T)\,\bar{\rho}_2 + (1-2x_T)^2\,\bar{\rho}_3\right]\end{aligned} \tag{13}$$

where $T_{ci}$ is the critical temperature of pure fluid $i$, similarly for $P_{ci}$ and $\rho_{ci}$, and

$$x_T = \frac{1/T_{c1} - 1/T_c(x)}{1/T_{c1} - 1/T_{c2}} \tag{14}$$

An alternate formulation [2, 4] replaces Eqs. (12) and (13) by polynomials in $x$ with unbarred coefficients $P_i$ and $\rho_i$, but this alternative is less advantageous for the mixtures considered here.

Knowledge of the pure fluid saturation properties and the critical line determines all parameters of the model except for the three adjustable parameters $C_H$, $C_X$, and $C_Z$. The experimental results analyzed here consist of dew-bubble curves (loci of constant $x_l$ and $x_v$ in the $P$–$T$ plane) and temperature-density coexistence curves at fixed composition. Construction of the corresponding theoretical loci requires a numerical inversion of Eq. (7). In our work, theoretical curves are calculated and displayed graphically by a minicomputer, and the parameters $C_H$, $C_X$, and $C_Z$ are optimized visually. Further details of the fitting methodology are described elsewhere [4].

The model is expected to provide a quality fit in the "critical region," $-0.1 < t < 0$, $0 \leqslant \zeta \leqslant 1$, and should not be used outside this region. It thus complements cubic equations of state such as the Peng–Robinson equation [6], which typically can be optimized for very accurate fits for $t < -0.1$ but, if so optimized, typically deviate from experiment significantly in the critical region.

All pure fluid parameters required for the present study have been tabulated elsewhere [3, 5, 7] with the exception of those of hexane. (Alkanes named here are understood to be their normal isomers unless otherwise indicated.) According to Young [8], for hexane $T_c = 507.95$ K and $P_c = 2.974$ MPa. Our previous policy has been to impose the constraints $C_3 = 30.0$ and $C_6 = 0$ for fluids, such as hexane, for which the critical divergence of the constant-volume specific heat is unavailable. Following this policy, we fit Young's data to Eqs. (3) and (6) and find that $\rho_c = 2.718$ kg-mol $\cdot$ m$^{-3}$, $C_1 = 2.071$, $C_2 = -0.971$, $C_4 = 6.519$, and $C_5 = -21.644$.

## 2. BUTANE–PENTANE

The results of our model as applied to the mixture butane–pentane are shown in Fig. 1. The experimental points are those published by Kay et al.

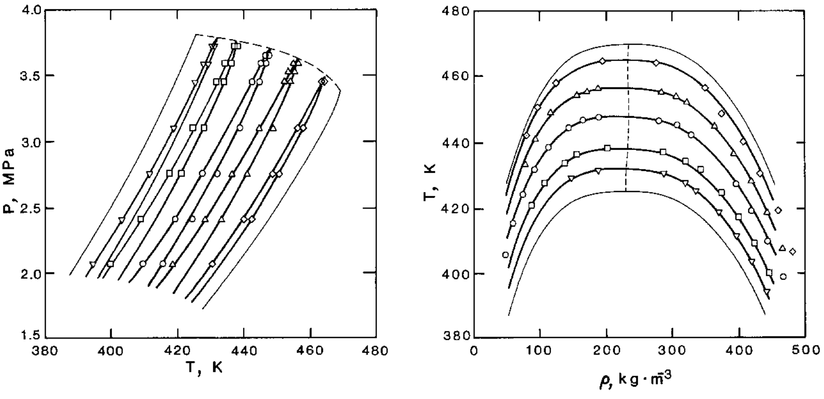

**Fig. 1.** Dew-bubble curves (a) and coexisting density curves (b) from the theory for butane–pentane. The dashed lines represent the model critical locus. Mole fractions of butane of the experimental data, from Ref. 9, are (◇) 0.1399, (△) 0.3493, (○) 0.5444, (□) 0.7518, and (▽) 0.8745.

[9] and are not the original, unpublished data points but, rather, the published smoothed data values at an evenly spaced set of pressures. The use of original data would be preferable, but at the present level of visual fitting the alternative of using smoothed data is not expected to alter the results substantially. Similar comments apply to our later fits of butane–hexane and ethane–butane. The theoretical curves for this and subsequent fits span the region $-0.09 < t < 0$.

Our model fits all data points in the critical region to within 0.7 K in temperature, 0.03 MPa in pressure, and $3\ \mathrm{kg \cdot m^{-3}}$ in density. Kay et al. [9] state a precision for their data of 0.5 K, 0.014 MPa, and $1\ \mathrm{kg \cdot m^{-3}}$ for liquid densities and $0.1\ \mathrm{kg \cdot m^{-3}}$ for vapor densities, with possibly larger uncertainties near the critical line.

Critical-line parameters are listed in Table I. The parameters of Eqs. (11)–(13) were obtained from a linear-regression fit of mixture critical points listed in Ref. 9 to those equations, subject to a few minor adjustments. Our critical line agrees with that of Kay et al. to within 0.35 K in temperature, 0.023 MPa in pressure, and $3.7\ \mathrm{kg \cdot m^{-3}}$ or 1.6% in density, given the assumption that the entry for $x = 0.5444$ in Table VII of Ref. 9 is misprinted as 0.2250 and should be 0.2350.

The optimal mixture parameters are found to be $C_\mathrm{H} = -6$, $C_\mathrm{X} = C_\mathrm{Z} = 0$. This result is typical of normal (i.e., nonazeotropic) mixtures with narrow dew-bubble curves, such as propane–butane [5] ($C_\mathrm{H} = -7$) and isobutane–isopentane [7] ($C_\mathrm{H} = -12$), where $C_\mathrm{X}$ and $C_\mathrm{Z}$ may be set equal to zero because they are not needed in the model. In fact, the simpler model first proposed by Moldover and Gallagher [2] (which is equivalent to the present model with $C_\mathrm{H} = C_\mathrm{X} = C_\mathrm{Z} = 0$ and thus predicts the coexistence surface, without adjustable parameters, directly from pure fluid

**Table I.** Critical-Line Parameters

| | Butane + pentane | Butane + hexane | Propane + isopentane | Ethane + butane |
|---|---|---|---|---|
| $T_1$ ($\mathrm{kg\text{-}mol \cdot MPa^{-1} \cdot m^{-3}}$) | $-8.066 \times 10^{-3}$ | $-2.556 \times 10^{-2}$ | $-3.692 \times 10^{-2}$ | $-9.233 \times 10^{-2}$ |
| $T_2$ ($\mathrm{kg\text{-}mol \cdot MPa^{-1} \cdot m^{-3}}$) | $-1.34 \times 10^{-5}$ | $8.36 \times 10^{-3}$ | $1.024 \times 10^{-2}$ | $3.465 \times 10^{-2}$ |
| $T_3$ ($\mathrm{kg\text{-}mol \cdot MPa^{-1} \cdot m^{-3}}$) | $-2.682 \times 10^{-3}$ | $-3.21 \times 10^{-3}$ | $-9.56 \times 10^{-3}$ | $-1.265 \times 10^{-2}$ |
| $\bar{P}_1$ ($\mathrm{kg\text{-}mol \cdot m^{-3}}$) | 0.1186 | 0.4054 | 0.7795 | 1.8849 |
| $\bar{P}_2$ ($\mathrm{kg\text{-}mol \cdot m^{-3}}$) | 0.07543 | 0.0329 | 0.1063 | 0.3011 |
| $\bar{P}_3$ ($\mathrm{kg\text{-}mol \cdot m^{-3}}$) | 0.07846 | $-0.0197$ | 0.1353 | 0.0435 |
| $\bar{\rho}_1$ ($\mathrm{kg\text{-}mol \cdot m^{-3}}$) | 0.2159 | 0.0511 | 0.661 | 2.0775 |
| $\bar{\rho}_2$ ($\mathrm{kg\text{-}mol \cdot m^{-3}}$) | $-0.1528$ | $-0.1089$ | $-1.088$ | $-0.5443$ |
| $\bar{\rho}_3$ ($\mathrm{kg\text{-}mol \cdot m^{-3}}$) | $-0.2955$ | 0.0956 | $-0.2485$ | 0.2636 |

saturation properties and the critical line) provides a fit for butane–pentane to within 1.3 K of the data, but those predictions quite clearly are systematically high in temperature.

## 3. BUTANE–HEXANE

The results of our model as applied to butane–hexane are shown in Fig. 2. Once again, the experimental points are smoothed data published by Kay et al. [9]. The model fits all data points in the critical region to within 1 K, 0.02 MPa, and $6\ \mathrm{kg \cdot m^{-3}}$, where the greatest deviation in density is at the edge of the critical region on the liquid side for $x = 0.7017$. The experimental precision, as stated by Kay et al., is the same as that for butane–pentane.

Critical-line parameters, listed in Table I, were again obtained from linear-regression fits of Eqs. (11)–(13) to mixture critical points listed in Ref. 9, followed by some minor adjustments. Our critical line agrees with that of Kay et al. to within 0.22 K in temperature, 0.016 MPa in pressure, and $3.6\ \mathrm{kg \cdot m^{-3}}$ or 1.6% in density.

The mixture parameters are $C_H = -9$, $C_X = 0.15$, and $C_Z = 0$. This result is typical of mixtures with medium-width dew-bubble curves, such as nitrogen–methane [4] ($C_H = -6$, $C_X = 0.3$) and propane–pentane [5] ($C_H = -6$, $C_X = 0.3$), where $C_Z$ is not needed in the model and thus is set equal to zero.

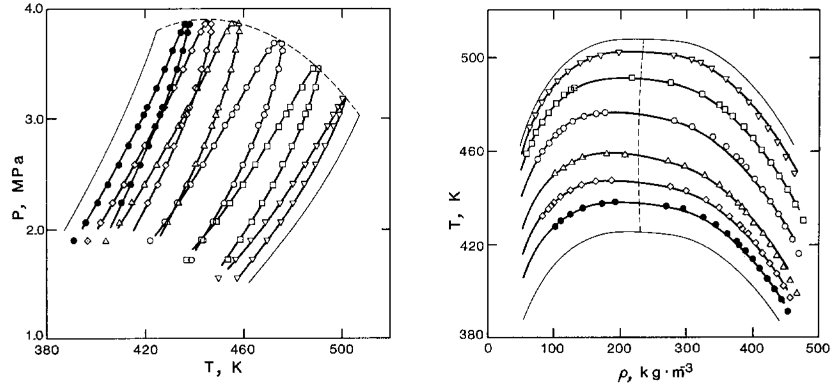

**Fig. 2.** Dew-bubble curves (a) and coexisting density curves (b) from the theory for butane–hexane. Mole fractions of butane of the experimental data, from Ref. 9, are (▽) 0.1035, (□) 0.2841, (○) 0.4928, (△) 0.7017, (◇) 0.8127, and (●) 0.899.

## 4. PROPANE–ISOPENTANE

The results of our model as applied to propane–isopentane are shown in Fig. 3. Experimental data are the original data points of Vaughan and Collins [10]. Unlike the other experimental measurements due to Kay and co-workers [9, 11] cited in this paper, data for propane–isopentane are sparse in the critical region. Vaughan and Collins provide only two or three measurements on each of the liquid and vapor sides for five compositions over the region $-0.09 \leqslant t \leqslant 0$.

Our model provides a quite reasonable correlation of these limited experimental results. There are two apparent outlier data points. The point $x = 0.794$, $T_c = 383.16$ K, $P = 4.088$ MPa, is high in pressure, compared to the model predictions, by 0.12 MPa, but is fit well on the $T$–$\rho$ graph. The point $x = 0.101$, $T = 398.16$ K, $\rho = 450.1$ kg · m$^{-3}$, is low in density, compared to the model predictions, by 23 kg · m$^{-3}$ or 5 %, although this point would be fit well by the model, if extended to lower $t$, on the $P$–$T$ graph.

Otherwise, the data are fit to within 1 K in temperature, 0.05 MPa in pressure, and 10 kg · m$^{-3}$ or 3 % in density. Vaughan and Collins state a precision of 0.02 K in temperature, 0.2 % in pressure at the highest pressures, and as much as "several per cent" in coexisting liquid volumes. They also state that their critical volumes "may be in error by several per cent." Our critical line agrees with theirs in temperature to within 0.68 K and in pressure to within 0.037 MPa but is systematically below theirs in

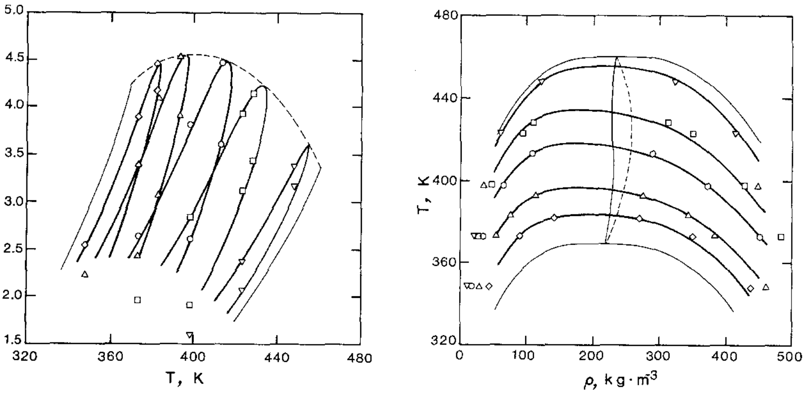

**Fig. 3.** Dew-bubble curves (a) and coexisting density curves (b) from the theory for propane–isopentane. On the temperature–density plot, the solid vertical curve is the model critical locus and the dashed curve is the critical locus according to Ref. 10. Mole fractions of propane of the experimental data, from Ref. 10, are (▽) 0.101, (□) 0.393, (○) 0.588, (△) 0.794, and (◇) 0.899.

density by as much as 12.1 % at $x = 0.393$. Both critical lines are graphed in Fig. 3b and our critical-line parameters are listed in Table I. As explained elsewhere for nitrogen–methane [4] and methane–ethane [5], we believe that in some cases our model can provide a more accurate critical line in density than that determined by direct experimental measurement.

The mixture parameters are $C_H = -6$, $C_X = 0.1$. Like butane–hexane, this result is typical of mixtures with medium-width dew-bubble curves. This fit provides an example of how our model can provide reasonable correlations from limited experimental data. A more thorough experimental investigation of VLE for propane–isopentane in the critical region would be desirable.

## 5. ETHANE-BUTANE

As a final example, the results of our model as applied to ethane–butane are shown in Fig. 4. Experimental points are smoothed data as published by Kay [11]. This mixture possesses wide dew-bubble curves qualitatively similar to other alkane mixtures with 2:1 carbon-number ratios and hence approximately 2:1 molecular mass ratios (e.g., methane–ethane [5] and butane–octane [4]), for which nonzero values for $C_Z$ are required. A subsequent experimental study of ethane–butane isotherms in *P–x* space by Mehra and Thodos [12] produced results in good agreement with those of Kay.

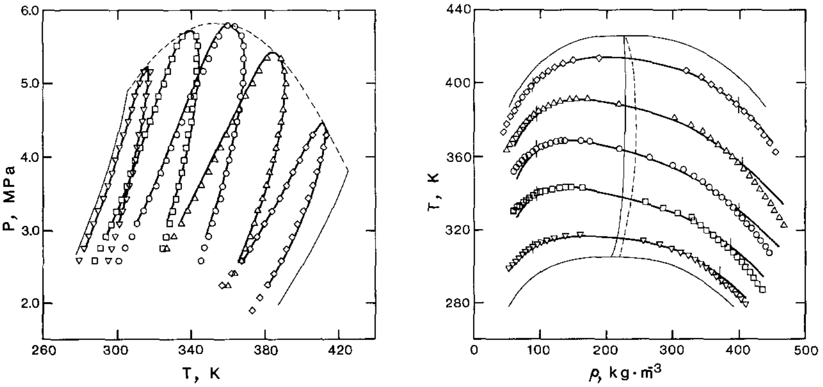

**Fig. 4.** Dew-bubble curves (a) and coexisting density curves (b) from the theory for ethane–butane. On the temperature–density plot, the solid vertical curve is the model critical locus, the dashed curve is the critical locus according to Ref. 11, and the small vertical bars locate where $t = -0.045$. Mole fractions of ethane of the experimental data, from Ref. 11, are (◇) 0.1749, (△) 0.541, (○) 0.6577, (□) 0.8218, and (▽) 0.9472.

Critical-region VLE data become increasingly difficult to fit as the dew-bubble curves become wider. Previous fit standards, nevertheless, are maintained here in the $P$–$T$ diagram, for which our model fits the data to within 1 K in temperature and 0.06 MPa in pressure. (Kay does not specify the experimental precision.) However, on the $T$–$\rho$ diagram, the model deviates from experiment toward high densities significantly and systematically away from the critical line.

The vertical bars on the theoretical curves in Fig. 4b locate the midpoints of the fitting region, i.e., where $t = -0.045$. Substantial deviations between theory and experiment of more than $3\ \mathrm{kg \cdot m^{-3}}$ occur only when $t < -0.045$, whereas over a "restricted critical region," $-0.045 \leqslant t \leqslant 0$, the fit in density is reasonable. The range of accurate representation of coexisting densities could probably be increased by adding to the model a quadratic $\zeta$ term in Eq. (4) for $C_2(\zeta)$, the slope of the "rectilinear diameter" as a function of zeta.

The mixture parameters are $C_H = -7$, $C_X = 0.45$, and $C_Z = -1.0$. This result is typical of normal mixtures with wide dew-bubble curves, such as butane–octane [4] ($C_H = -12$, $C_X = 0.3$, $C_Z = -1.3$) and methane–ethane [5] ($C_H = -7$, $C_X = 0.5$, $C_Z = -1.4$). Similar difficulties in fitting coexisting densities away from critical have been experienced with those mixtures also [4, 5].

Critical-line parameters are listed in Table I. Our critical line agrees with Kay's to within 0.32 K in temperature and 0.038 MPa in pressure, with the greatest pressure deviation for pure ethane. The critical densities differ by as much as $13\ \mathrm{kg \cdot m^{-3}}$ or 6%, in part because Kay's critical density for pure ethane ($220\ \mathrm{kg \cdot m^{-3}}$) differs from the presently accepted value ($207\ \mathrm{kg \cdot m^{-3}}$). As explained in Ref. 5, for mixtures with wide dew-bubble curves the model critical densities may differ from the actual critical densities by 2 or 3%, although the critical densities quoted in experimental papers can be even more in error.

## 6. SUMMARY

Using the modification of the Leung–Griffiths [1] theory of Rainwater and Moldover [2–5] for critical-region VLE, we have successfully fit data in temperature, pressure, and density for the mixtures butane–pentane, butane–hexane, propane–isopentane, and ethane–butane over the region $-0.09 \leqslant t \leqslant 0$, except that coexisting densities for ethane–butane are adequately represented only over the region $-0.045 \leqslant t \leqslant 0$. This work brings to 14 the total number of mixtures whose critical-region VLE behavior has been successfully fit by the original [1, 13, 14] or modified [2, 4–6, 15] Leung–Griffiths method.

We are in the process of developing a user-friendly minicomputer program package to implement our model, with which the user can easily calculate phase equilibrium curves for compositions other than those experimentally measured and can employ the model to fit data for new mixtures.

## ACKNOWLEDGMENTS

The authors acknowledge the extensive theoretical and computational contributions of M. R. Moldover which form the basis of the present work. They thank I. Vázquez Pantoja for bibliographic and computational assistance and K. Bowie for typing the paper.

## REFERENCES

1. S. S. Leung and R. B. Griffiths, *Phys. Rev.* **A8**:2670 (1973).
2. M. R. Moldover and J. S. Gallagher, *AIChE J.* **24**:267 (1978).
3. J. C. Rainwater, Natl. Bur. Stand. (U.S.) Technical Note 1061, p. 83 (1983).
4. J. C. Rainwater and M. R. Moldover, in *Chemical Engineering at Supercritical Fluid Conditions*, M. E. Paulaitis, et al., eds. (Ann Arbor Science, Ann Arbor, Mich., 1983), p. 199.
5. J. C. Rainwater, I. Vázquez Pantoja, and M. R. Moldover, to be published.
6. D. Y. Peng and D. B. Robinson, *I & EC Fund.* **15**:59 (1976).
7. D. E. Diller, J. S. Gallagher, B. Kamgar-Parsi, G. Morrison, J. C. Rainwater, J. M. H. Levelt Sengers, J. V. Sengers, L. J. Van Poolen, and M. Waxman, Natl. Bur. Stand. (U.S.) Interagency Report 85-3124 (1985).
8. S. Young, *Proc. Roy. Soc. Dublin* **12**:374 (1910).
9. W. B. Kay, R. L. Hoffman, and O. Davies, *J. Chem. Eng. Data* **20**:333 (1975).
10. W. E. Vaughan and F. C. Collins, *Ind. Eng. Chem.* **34**:885 (1942).
11. W. B. Kay, *Ind. Eng. Chem.* **32**:353 (1940).
12. V. S. Mehra and G. Thodos, *J. Chem. Eng. Data* **10**:307 (1965).
13. G. D'Arrigo, L. Mistura, and P. Tartaglia, *Phys. Rev.* **A12**:2587 (1975).
14. R. F. Chang and T. Doiron, *Int. J. Thermophys.* **4**:337 (1983).
15. T. A. Al-Sahhaf, E. D. Sloan, and A. J. Kidnay, *AIChE J.* **30**:867 (1984).